Preprint
UCRL-JC- 152695

Effect of Profiles and Shape on Ideal Stability of Advanced Tokamak Equilibria

M. A. Makowski, T. A. Casper, J. R. Ferron, T. S. Taylor, A. D. Turnbull

This article was submitted to: *30th EPS Conference on Controlled Fusion and Plasma Physics, St. Petersburg, Russia 07/07/2003 – 07/11/2003*

U.S. Department of Energy

Lawrence Livermore National Laboratory

July 7, 2003

This work was performed under the auspices of the U.S. Department of Energy by University of California, Lawrence Livermore National Laboratory under Contract W-7405-Eng-48.

Effect of Profiles and Shape on Ideal Stability of Advanced Tokamak Equilibria

M.A. Makowski[1], T.A. Casper[1], J.R. Ferron[2], T.S. Taylor[2], and A.D. Turnbull[2]

[1] *Lawrence Livermore National Laboratory, Livermore, California, 94550 USA*
[2] *General Atomics, P.O. Box 85608, San Diego, California 92186-5608 USA*

Abstract. The pressure profile and plasma shape, parameterized by elongation (κ), triangularity (δ), and squareness (ζ), strongly influence stability. In this study, ideal stability of single null and symmetric, double-null, advanced tokamak (AT) configurations is examined. All the various shapes are bounded by a common envelope and can be realized in the DIII-D tokamak. The calculated AT equilibria are characterized by $P_0/\langle P \rangle \sim$ 2.0–4.5, weak negative central shear, high q_{min} (>2.0), high bootstrap fraction, an H-mode pedestal, and varying shape parameters. The pressure profile is modeled by various polynomials together with a hyperbolic tangent pedestal, consistent with experimental observations. Stability is calculated with the DCON code and the resulting stability boundary is corroborated by GATO runs.

1. Introduction

Plasma boundary shape and the pressure profile are both known to strongly influence global stability. These parameters are especially important in advanced tokamak (AT) configurations. The effect of boundary shape and pressure profile is systematically studied with the aim of obtaining the optimal β_N.

We start with a specified pressure profile composed of a polynomial for the core plus a hyperbolic tangent function for the pedestal. The pressure peaking factor, $P_0/\langle P \rangle$, is varied by varying b_n in the polynomial, $P_n'(\psi) = -P_{0n}'[\,1 + b_n\,\psi - (\,1 + b_n)\,\psi^2\,]$ where ψ is the normalized poloidal flux, P_n' is the derivative of the pressure profile, and $-P_{0n}'$ is its value at $\psi = 0$. The additive hyperbolic tangent function uses a pedestal pressure derived from a scaling law based on an experimental fit to DIII-D data. Model temperature and density profiles are then derived consistent with the pressure profile. The bootstrap current is computed using the NCLASS formulation together with the temperature and density profiles. A seed current that fills in the current profile at the center is added to the bootstrap current to fully specify the current profile. The seed current also has the effect of fixing q_0 and is such as to produce weak negative central shear in the resulting q-profile.

Before the equilibrium can be obtained the boundary must be specified. A boundary of the form $R = R_0 + a\cos[\theta + \sin^{-1}\delta \sin\theta]$, $z = \kappa\, a \sin[\theta + \zeta_{o,i}\sin(2\theta)]$, where R_0 is the major radius, a is the minor radius, δ the triangularity, κ the elongation, and $\zeta_{o,i}$ are the outer and inner squareness. Having the pressure and current profiles specified together with the boundary, it is possible to solve for the equilibrium using the TEQ package in CORSICA. The resulting equilibria possess the following general characteristics of AT discharges: weak negative central shear with high q_{min} ($q_0 \sim$ 2.5–2.7 and $q_{min} \sim$2.1–2.4), $f_{BS} \sim$ 0.70–0.95, $I_p \sim$ 0.9–1.1 MA, and an H-mode edge pedestal.

Once the equilibrium has been computed, stability analysis is performed. n = 1 and 2 ideal stability is calculated within CORSICA using the DCON package. Ballooning stability is evaluated using a ballooning package also contained within CORSICA. The GATO ideal stability code is also used to crosscheck n = 1, 2 stability. For all stability calculations, an ideal conducting wall at the location of the DIII-D vacuum vessel is assumed. The various stability limits are found by incrementing the central pressure and repeating the above procedure. The entire process is repeated for each polynomial and value of shape parameter (κ, δ, and ζ_o). The parameter space encompassed by this study is κ = 1.8, 1.9, 2.0; δ = 0.5, 0.65, 0.8; ζ_o = 0.0, 0.1, 0.2, and six polynomials (b_n = –2, –5/3, –4/3, –1, –1/2, 1; the profile broadens with increasing b_n) yielding a range of peaking factors of 2.0–4.5.

2. Stability Limits for Symmetric AT Equilibria

Figure 1(a,b) shows the global stability results. Figure 1(a) plots the n = 1 beta limit as a function of the pressure peaking factor, $P_0/\langle P\rangle$ for the entire data set. In this case the maximum β_N clearly increases inversely with the peaking factor. A power law fit to the data is also shown in the plot and yields a relatively strong dependence on the peaking factor of $(P_0/\langle P\rangle)^{-1.32}$. Similarly, Fig. 1(b) plots the n = 2 beta limit. Here, the envelope of maximum β_N values also scales inversely with the peaking factor. However, due to the large variation with shape parameters, an exponent could not be inferred. At large peaking factors the limiting β_N tends to result from the n = 1 mode, while at low peaking factors, it results from the n = 2. The crossover between the n = 1 and 2 occurs at a peaking factor ~2.5.

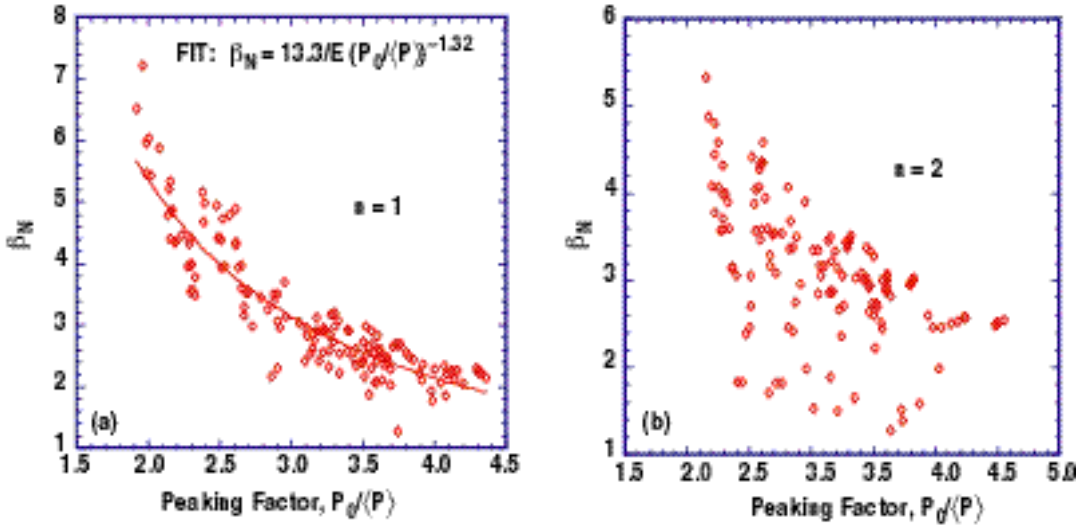

Fig. 1. Limiting β_N values for the n = 1 (a) and n = 2 (b) ideal modes as a function of $P_0/\langle P\rangle$ for all combinations of κ, δ, ζ_o, and peaking factor.

The lower values of β_N for the n = 2 mode (in the range 1.5–2.5) generally correspond to a first-stability limit for equilibria with shape parameters at the extremes of the their ranges, such as δ = 0.8 with ζ_0 = 0.0. As the pressure is increased, the n = 2 mode generally stabilizes and a second n = 2 limit is encountered in the β_N range of 3–5. In Fig. 1(b) only the lower of these two value of the n = 2 β-limit is plotted. The variation in the

data is higher than for the n = 1 mode and increases with decreasing peaking factor. This remains true even if the lower β_N values are ignored. In general, the n = 1 limit is dominated by profile effects, whereas shape plays a more significant role with respect to the n = 2 limit, with the highest β_N values at a given peaking factor occurring for an optimal shape

Two ballooning unstable regions were often found to exist. The lower ballooning beta limit was found to be uniformly in the range 2.7–3.0 except at the lowest peaking factor where it increased abruptly to 5.5 for a restricted set of shapes.

As is evident in Fig. 1 there is a large variation in the data at any particular value of the peaking factor. This results from the complicated dependence of the beta limit on the shape factors, δ, κ, and ζ_o, as well as on the details of the pressure profile through b_n as shown in Fig. 2. Here the n = 1 and 2 limits are plotted versus δ (at fixed κ, ζ_o, and peaking factor) and versus ζ_o (at fixed κ, δ, and peaking factor). For the δ-scan of Fig. 2(a), the maximum β_N is limited everywhere by the n = 1 mode. In contrast, for the ζ_o-scan of Fig. 2(b), the β-limit is set everywhere by the n = 2 mode. The n = 1 δ-scan shows an optimal intermediate value of $\delta \sim 0.6$, whereas the n = 2 ζ_o-scan is monotone decreasing with ζ_o. For the δ-scan, an n = 1 internal mode actually sets the β-limit at $\delta = 0.8$.

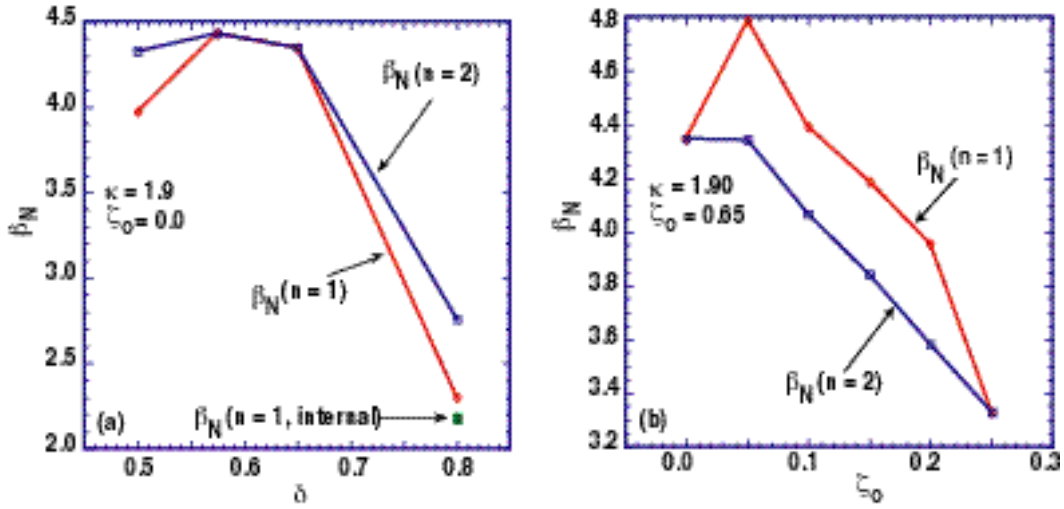

Fig. 2. Parameter scans of maximum β_N vs δ at fixed κ and ζ_o (a) and vs ζ_o at fixed κ and δ. The peaking factor is ~2.5 for both (a) and (b).

Figure 3 shows a parameter scan of β-limit for the n = 1 and 2 modes versus κ for several values of ζ_o at fixed δ and peaking factor. The n = 2 mode always sets the β-limit. Again the parametric dependence is complicated. Increasing κ leads to a higher β-limit except at the largest squareness. Considering all cases the β-limit is 4.6 for a peaking factor of ~2.5 with $\kappa = 2.0$, $\delta = 0.65$, and $\zeta_o = 0$, and results from an n = 2 mode.

The ideal stability code GATO was used to check some of the DCON results presented here. For the six cases studied, corresponding to the ζ_o parameter scan of Fig. 2(b), the β-limits either agree exactly or differ by at most 10%, with DCON generally predicting a slightly higher β-limit than GATO.

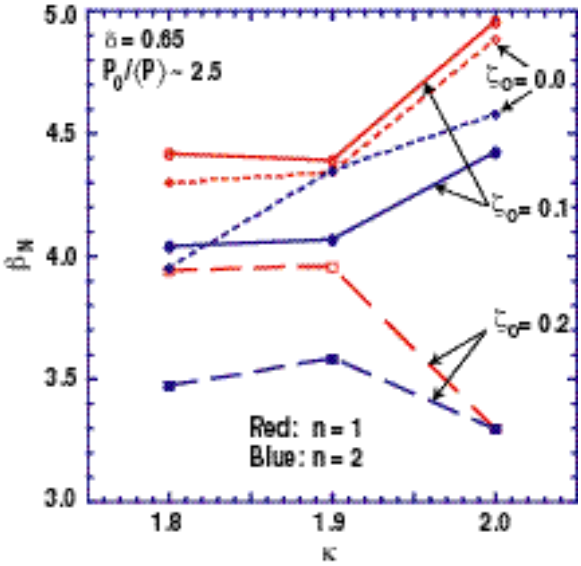

Fig. 3. Parameter scan of maximum β vs κ at fixed δ and peaking parameter

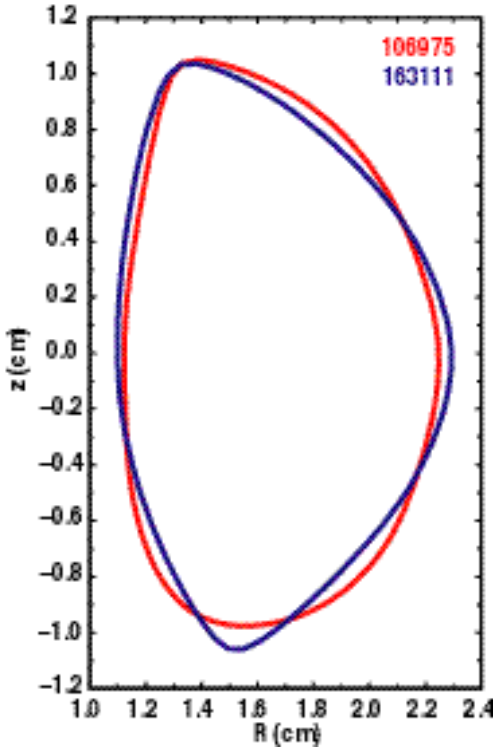

Fig. 4. Asymmetric equilibria optimized to couple of the upper (106975) and lower (163111) divertors in DIII-D.

3. Stability Limits of Asymmetric Equilibria

In addition to the above previously discussed equilibria, the ideal stability of some up/down asymmetric equilibria was also examined. Two such shapes are shown in Fig. 4. These shapes are chosen to couple to the upper (106975) and lower (163111) divertors in DIII-D. (The latter is only a proposed shape at this time, whereas the former has been used in experiments). Stability analysis of these equilibria yields the following β-limits corresponding to a peaking factor of ~2.5. For 106975 the β_N-limits are 2.67, 2.98, and 2.98 respectively for the n = 1, 2, and ballooning modes (limiting value is β_N = 2.67). Similarly, for 163111 the β-limits are 3.85, 3.85, and 4.59 respectively (limiting β_N = 3.85). Both limiting βs for these specific shapes are ~25% below the optimum found above for the symmetric equilibria

4. Conclusions

Plasma boundary shape and the pressure profile are important for determining global plasma stability. The pressure profile plays a significant role in setting the β-limits for the n = 1 and 2 modes, particularly the former. Shape plays a greater role in setting the n = 2 stability limit. The optimum β is a complex function of the shape parameters κ, δ, and ζ_o. GATO and DCON agree quite well on both the n = 1 and 2 stability limits. This fact has made this study possible as stability analysis of all the cases with GATO alone would have been prohibitive in terms of time

Work supported by U.S. Department of Energy under Contract DE-AC03-99ER54463, and Grants DE-FG03-97ER54415, DE-FG02-92ER54141, DE-FG03-96ER54373, and DE-FG03-01ER54615.